

Check for updates



TaSPX3 Enhances Wheat Resistance to Leaf Rust by Antagonising TaDi19-Mediated Repression of Pathogenesis-Related Genes

Huimin Qian¹ | Chuang Li^{1,2} | Yanan Lu¹ | Xue Li² | Jianping Zhang² | Junyi Zhao¹ | Keyan Wu¹ | Yanyan Zhang¹ | Kun Cheng¹ | Daowen Wang² | Pengyu Song¹ | Na Liu¹ | Wenming Zheng¹ |

¹Key Laboratory of High-Efficiency Production of Wheat-Maize Double Cropping, College of Life Sciences, Henan Agricultural University, Zhengzhou, China | ²Key Laboratory of High-Efficiency Production of Wheat-Maize Double Cropping, College of Agronomy, Henan Agricultural University, Zhengzhou, China

Correspondence: Pengyu Song (pysong@henau.edu.cn) | Na Liu (naliu@henau.edu.cn) | Wenming Zheng (wmzheng@henau.edu.cn)

Received: 20 May 2025 | Revised: 8 September 2025 | Accepted: 24 September 2025

Funding: This study was supported by the National Natural Science Foundation of China (32400243), the Henan Provincial Science and Technology Major Project (221100110100), the National Key Research and Development Program of China (2021YFF1000203), the Research start-up fund to top-notch talents of Henan Agricultural University (30500924), and the Postdoctoral Fellowship Program of CPSF (GZC20230717).

Keywords: leaf rust | PTI | TaDi19 | TaPRs | TaSPX3 | wheat

ABSTRACT

Wheat leaf rust, caused by *Puccinia triticina* (*Pt*), threatens global wheat production, with yield losses further exacerbated by the pathogen's evolving virulence. Although Syg1/Pho81/Xpr1 (SPX) domain-containing proteins are known regulators of phosphate homeostasis, their involvement in plant–pathogen interactions remains largely unexplored. We demonstrated that *TaSPX3*, a wheat SPX family gene, is rapidly induced during early *Pt* infection and flg22 treatment. Genetic evidence indicates that *TaSPX3* is a positive regulator of rust resistance, with knockdown lines showing increased susceptibility and overexpression lines exhibiting enhanced resistance. Using yeast two-hybrid screening, we identified TaDi19-1D, a zinc finger transcription factor, as a direct TaSPX3 interactor. TaDi19-1D functions as a negative immune regulator by suppressing the expression of pathogenesis-related (PR) genes (*TaPR1*, *TaPR2*, *TaPR5*) through direct promoter binding. TaSPX3 counteracts this repression by physically interacting with TaDi19-1D, thereby derepressing PR gene expression and boosting wheat resistance to *Pt*. Our findings revealed a novel TaSPX3–TaDi19 regulatory module that fine-tunes *TaPRs* expression, providing mechanistic insights into pattern-triggered immunity (PTI) and potential genetic targets for breeding durable broad-spectrum disease-resistant wheat varieties.

1 | Introduction

Wheat leaf rust, caused by the obligate biotrophic fungus *Puccinia triticina* (*Pt*), remains a major constraint to global wheat production, causing annual yield losses of approximately 5%–15% globally (Ali et al. 2022; Gultyaeva et al. 2023; Hassan et al. 2022). Although resistant cultivars offer the most sustainable control strategies (Zhao and Kang 2023), the effectiveness of race-specific resistance genes is frequently overcome through pathogen evolution (Kumar et al. 2024; Zhang et al. 2020). This

highlights the urgent need to identify novel resistance mechanisms, particularly those involving broad-spectrum immune components, which are less vulnerable to pathogen adaptation (Li et al. 2019; Sun et al. 2024; Wang et al. 2022).

SPX domain-containing proteins, named after the conserved Syg1/Pho81/Xpr1 domain, play pivotal roles in phosphate homeostasis across eukaryotes (Legati et al. 2015; Wild et al. 2016). In plants, these proteins that contain only the SPX domain regulate phosphorus signalling primarily through interactions

This is an open access article under the terms of the Creative Commons Attribution-NonCommercial-NoDerivs License, which permits use and distribution in any medium, provided the original work is properly cited, the use is non-commercial and no modifications or adaptations are made.

© 2025 The Author(s). Plant Biotechnology Journal published by Society for Experimental Biology and The Association of Applied Biologists and John Wiley & Sons Ltd

with PHR transcription factors (Hu et al. 2019; Shi et al. 2014). Emerging evidence suggests that SPX proteins may also function in biotic stress responses, with rice SPX proteins modulating the trade-off between growth and blast disease resistance (He et al. 2024; Kong et al. 2021). Notably, fungal pathogens have evolved mechanisms to subvert SPX-mediated defences, as demonstrated by Magnaporthe's Nudix effectors that disrupt SPX-PHR interactions (McCombe et al. 2025; Qiu et al. 2025). Despite these advances, the immunological functions of the SPX proteins in wheat remain unknown.

Plant immunity against biotrophic pathogens involves a sophisticated two-layered defence system. Pattern-triggered immunity (PTI), which is activated upon recognition of pathogen-associated molecular patterns (PAMPs), provides broad-spectrum resistance through conserved signalling networks (Ngou et al. 2024; Wang and Kawano 2024; Yu et al. 2024). Key PTI responses include the induction of pathogenesis-related (PR) genes encoding antimicrobial proteins such as CAP-domain proteins (PR1), β-1,3-glucanases (PR2), thaumatin-like (PR5) (Couto and Zipfel 2016; Li et al. 2024; Liu and Ekramoddoullah 2006). The expression of these defence genes is tightly controlled by transcriptional regulators; for instance, phosphorylation of TGA3 enhances its association with NPR1 to activate PR genes (Han et al. 2022), whereas negative regulators such as TaPsIPK1 suppress PTI responses in wheat (Wang et al. 2022). However, the mechanism by which PR gene expression is modulated during wheat-rust interactions remains poorly understood.

In the present study, we identified *TaSPX3* as a novel positive regulator of leaf rust resistance in wheat. We demonstrated that TaSPX3 physically interacts with TaDi19-1D, a zinc finger transcription factor that represses TaPR gene expression. Our results revealed a previously unknown immune regulatory module in which TaSPX3 counteracts TaDi19-mediated transcriptional repression to activate PTI responses. These findings not only advance our understanding of wheat immunity but also provide valuable genetic resources for developing durable broadspectrum resistant wheat varieties through molecular breeding approaches.

2 | Results

2.1 | TaSPX3 Is Strongly Induced by Pt Infection and flg22 Treatment

Based on our previous identification of *TaSPX3* as a wheat homologue of *AtSPX3* (Liu et al. 2018) and its role in rust resistance (Na et al. 2024; Zhang et al. 2021), we investigated the transcriptional regulation of *TaSPX3* during pathogen infection. Quantitative reverse transcription polymerase chain reaction (qRT-PCR) analysis revealed striking induction patterns in both compatible (CS, Chinese Spring; Fielder) and incompatible (YM34, Yunmai 34) interactions with *Pt*15.

In the incompatible interaction, *TaSPX3* expression peaked dramatically at 12h post inoculation (hpi), showing approximately 21-fold induction compared to that in the mock-treated controls (0hpi), followed by sustained approximately 2-fold upregulation at 24 and 48 hpi (Figure 1A). The compatible interaction

exhibited a more moderate but consistent induction pattern, with a <6-fold upregulation observed at all time points examined (12, 24, 48 hpi) in CS and Fielder (Figure 1A). These results demonstrate that *TaSPX3* responds to *Pt* infection in both resistant and susceptible wheat lines.

To determine whether *TaSPX3* participates in PTI, we analysed its expression after treatment with flg22, a well-characterised PAMP. Notably, *TaSPX3* transcript levels were significantly elevated from 6 to 12h post-treatment (hpt) in all three genetic backgrounds (Figure 1B). This sustained upregulation suggests that *TaSPX3* is not only involved in specific resistance responses but may also play a role in broader PAMP-triggered defence signalling.

2.2 | *TaSPX3* Modulates Wheat Resistance to *Pt* Through Defence Gene Regulation

To elucidate the functional significance of *TaSPX3* in wheat defence against *Pt*, we established stable RNAi transgenic lines of the wheat cultivar Fielder. Three *TaSPX3*-RNAi lines (RNAi-L3, RNAi-L7, RNAi-L18) with confirmed *TaSPX3* knockdown (Figure S1) were subjected to a pathogen challenge. Complementary gain-of-function studies were conducted using three independent overexpression lines (OE-L16, OE-L29, OE-L30; Figure S2).

In the loss-of-function studies, three independent *TaSPX3*-RNAi lines (L3/7/18) exhibited compromised resistance, showing significantly larger uredinia (Figure 1C,D) and increased fungal biomass (Figure 1E) compared to those of the wild-type (WT) Fielder at 12 days post inoculation (dpi) with *Pt*15. Conversely, gain-of-function analysis using overexpression lines (OE-L16/29/30) revealed enhanced resistance, with markedly smaller infection areas and reduced pathogen biomass (Figure 1C–E). Microscopic examination of fungal development showed striking contrasts: RNAi plants supported longer hyphae (24 hpi) and expanded colonisation (48–120 hpi), whereas OE lines restricted hyphal growth and infection spread (Figure 1F–I).

Phenotypic differences correlated precisely with defence gene expression patterns. *TaSPX3* silencing significantly attenuated *Pt*-induced expression of the PR genes *TaPR1/2/5*, whereas over-expression boosted their basal and *Pt*-induced transcript levels (Figure 1J–L). Notably, the defence gene expression changes preceded visible symptom differences, suggesting *TaSPX3* operates early in immune signalling. These complementary genetic approaches established that *TaSPX3* positively regulates wheat resistance to leaf rust, likely by modulating PR gene-mediated defence pathways.

2.3 | TaSPX3 Confers Broad-Spectrum Disease Resistance in Wheat Without Affecting Agronomic Traits

To evaluate the role of *TaSPX3* in wheat growth and disease resistance, we compared the agronomic traits between *TaSPX3* transgenic lines and WT Fielder under controlled greenhouse conditions. No significant differences were observed in the

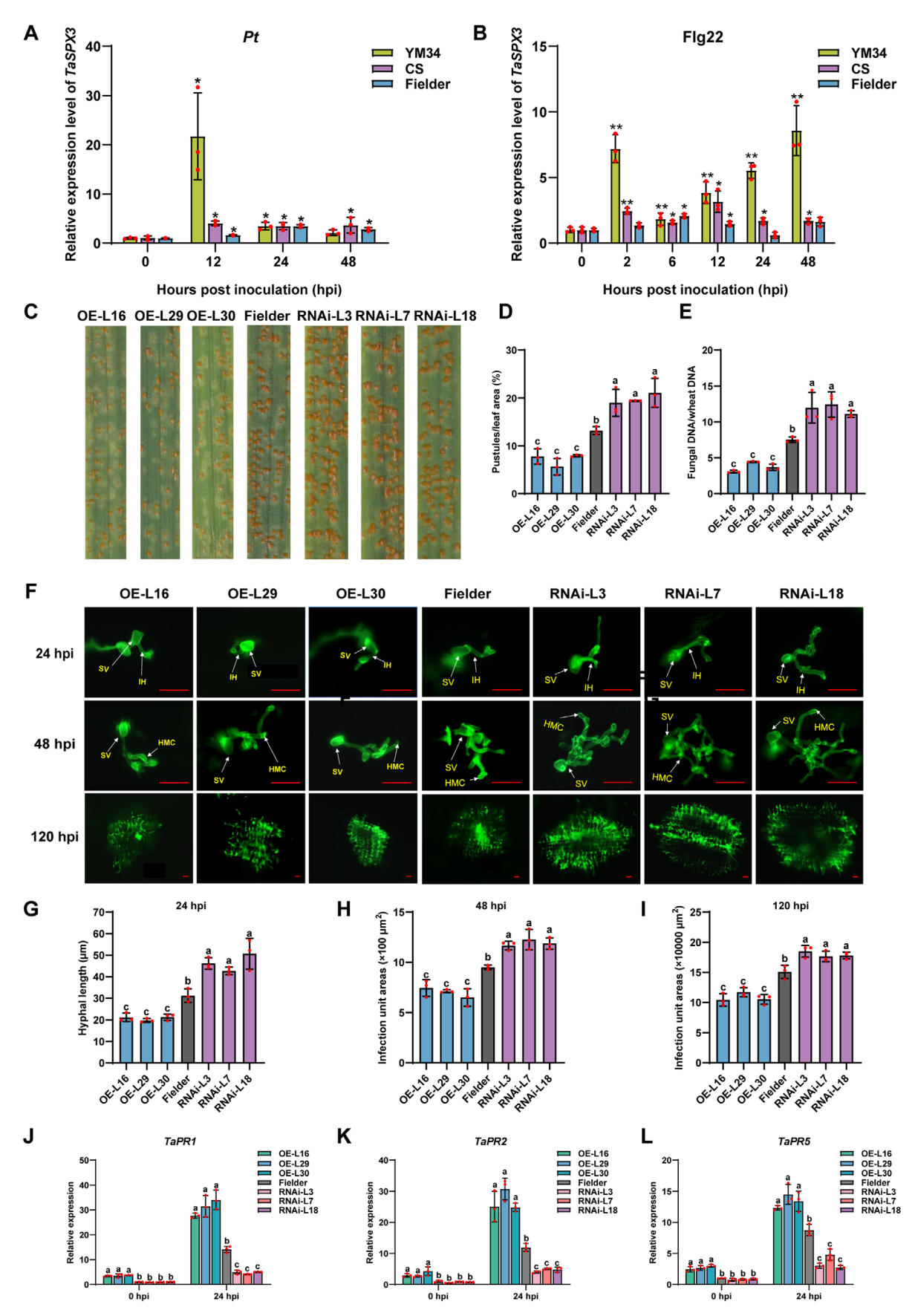


FIGURE 1 | Legend on next page.

FIGURE 1 | TaSPX3 positively regulates wheat leaf rust resistance. (A, B) Expression patterns of TaSPX3 in wheat leaves during $Puccinia\ triticina\ (Pt)$ infection (A) and flg22 treatment (B). Samples from CS, Fielder (compatible interaction), YM34 (incompatible interaction) following inoculation with Pt15 were collected at 0, 12, 24, 48 hpi. qRT-PCR was used to test relative expression levels from three biological replicates. Asterisks indicate significant differences between the column and 0 hpi of the corresponding variety using Student's t-test (*p<0.05, **p<0.01). (C, D) Disease symptoms and spore coverage quantification of TaSPX3-OE, WT, TaSPX3-RNAi plants infected with Pt15 at 12 dpi. (E) Fungal biomass in (C) estimated using qPCR. (F) Pt development in OE, WT, RNAi plants. Wheat leaves inoculated with Pt15 were sampled at 24, 48, and 120 hpi. Infection structures of Pt were stained with wheat germ agglutinin conjugated to Alexa-488. HMC, haustorial mother cell; IH, infection hypha; SV, substomatal vesicle. Scale bar, 20 μ m. (G–I) Hyphal length at 24 hpi (G) and infection areas at 48 (H) and 120 hpi (I). Data are represented as the mean \pm SD from at least 30 sites of three replicates. Scale bars, 20 μ m. (J–L) Relative expression of TaPR1, TaPR2, TaPR5 in OE, WT, RNAi plants. Leaves inoculated with Pt15 were sampled at 24 hpi. In D, E, G–L, distinct letters indicate significant differences (one-way ANOVA, Tukey's HSD test).

measured growth parameters between transgenic and WT plants (Figures S1E–J and S2E–J), indicating that *TaSPX3* manipulation did not affect normal wheat development.

To investigate whether *TaSPX3* mediates PTI-like broad-spectrum resistance, we challenged plants with two additional *Pt* isolates (*Pt*23 and *Pt*24), together with two *Blumeria graminis* f. sp. *tritici* isolates (JZ-WLQ-3 and SQ-YCS-3). Silencing of *TaSPX3* increased susceptibility to leaf rust, whereas OE lines showed significantly enhanced resistance compared to that of the WT controls (Figure S3). Consistent with the PTI characteristics, *TaSPX3* overexpression also conferred resistance against both tested powdery mildew isolates (Figure S4). These findings demonstrate that *TaSPX3* functions as a positive regulator of broad-spectrum disease resistance in wheat while maintaining normal agronomic performance.

2.4 | TaSPX3 Physically Interacts With Transcription Factor TaDi19-1D

To elucidate the molecular mechanisms underlying *TaSPX3*-mediated immune responses, we performed a yeast two-hybrid screen using a cDNA library derived from *Pt*-infected wheat leaves. This screening identified 18 potential TaSPX3-interacting proteins (Table S1), including TaDi19-1D (*TraesFLD1D01G441100*), a zinc finger transcription factor known to regulate PR gene expression in response to both biotic and abiotic stresses (Liu et al. 2013; Zhu et al. 2024). Subsequent validation through pairwise yeast two-hybrid assays confirmed the physical interaction between TaSPX3 and TaDi19-1D in yeast cells, as evidenced by the growth of cotransformed Y2HGold strains on selective media (Figure 2A). Among the tested homoeologs, TaDi19-1B, but not TaDi19-1A, exhibited similar binding activity to TaSPX3 (Figure S5).

This interaction was further substantiated using multiple experimental approaches. In vitro pull-down assays demonstrated specific binding between MBP-tagged TaDi19-1D and Myctagged TaSPX3, whereas control assays with MBP alone showed no interaction (Figure 2B). Subcellular localisation studies in *Nicotiana benthamiana* epidermal cells revealed that both proteins were localised in the cytoplasm and nucleus (Figure S6). Bimolecular fluorescence complementation assays showed that the interaction occurred specifically in the nucleus, with the YFP fluorescence signals detected exclusively in the nuclei of cells co-expressing nYFP-TaSPX3 and cYFP-TaDi19-1D (Figure 2C). Additional confirmation was obtained from split-luciferase complementation assays, which further verified this interaction *in*

planta (Figure 2D). These comprehensive analyses demonstrate that TaSPX3 specifically interacts with TaDi19-1D both in vitro and in vivo. Nuclear localisation of this interaction suggests potential transcriptional regulatory functions in plant immunity, providing mechanistic insights into *TaSPX3*-mediated defense responses against wheat leaf rust.

2.5 | *TaDi19* Expression in Wheat Is Dynamically Modulated by *Pt* Infection and flg22 Perception

To characterise the involvement of TaDi19 in wheat defence responses, we performed comprehensive expression profiling under both compatible and incompatible Pt infections, as well as flg22 treatment. The qRT-PCR analysis revealed distinct expression patterns during compatible and incompatible interactions with Pt. In susceptible (compatible) interactions, TaDi19 transcript levels showed progressive upregulation, reaching > 4-fold induction at 48 hpi in CS and 24 hpi in Fielder (Figure 3A). This induction pattern was completely absent in the resistant (incompatible) interactions, in which TaDi19 expression remained statistically unchanged throughout the course of infection.

The response to flg22 treatment exhibits an even more complex temporal regulation. Both interaction types displayed an initial suppression phase with significant downregulation observed at 2 hpt. However, a dramatic divergence emerged at 12 hpt, where incompatible interactions showed an approximately 12-fold increase in TaDi19 expression compared to that at baseline levels. This robust induction contrasted sharply with the modest approximately 2-fold increase observed in CS and no significant change in Fielder (Figure 3B). Collectively, these results demonstrated that TaDi19 expression in wheat is dynamically modulated by Pt infection and flg22 perception. The temporal precision and interaction-specific nature of these expression changes strongly implicate TaDi19 in the regulation of wheat immune responses.

2.6 | Silencing *TaDi19* Enhances Wheat Resistance Against *Pt*

To explore the role of *TaDi19* in wheat resistance to leaf rust, we performed virus-induced gene silencing (VIGS) targeting *TaDi19* (all three homologues) in two wheat cultivars, Fielder and Zhengmai 9023 (ZM9023), using barley stripe mosaic virus (BSMV). Control experiments with BSMV:*TaPDS* plants showed expected photobleaching phenotypes (Figure 3C and Figure S7A). qRT-PCR analysis verified a significant reduction in *TaDi19* transcript levels

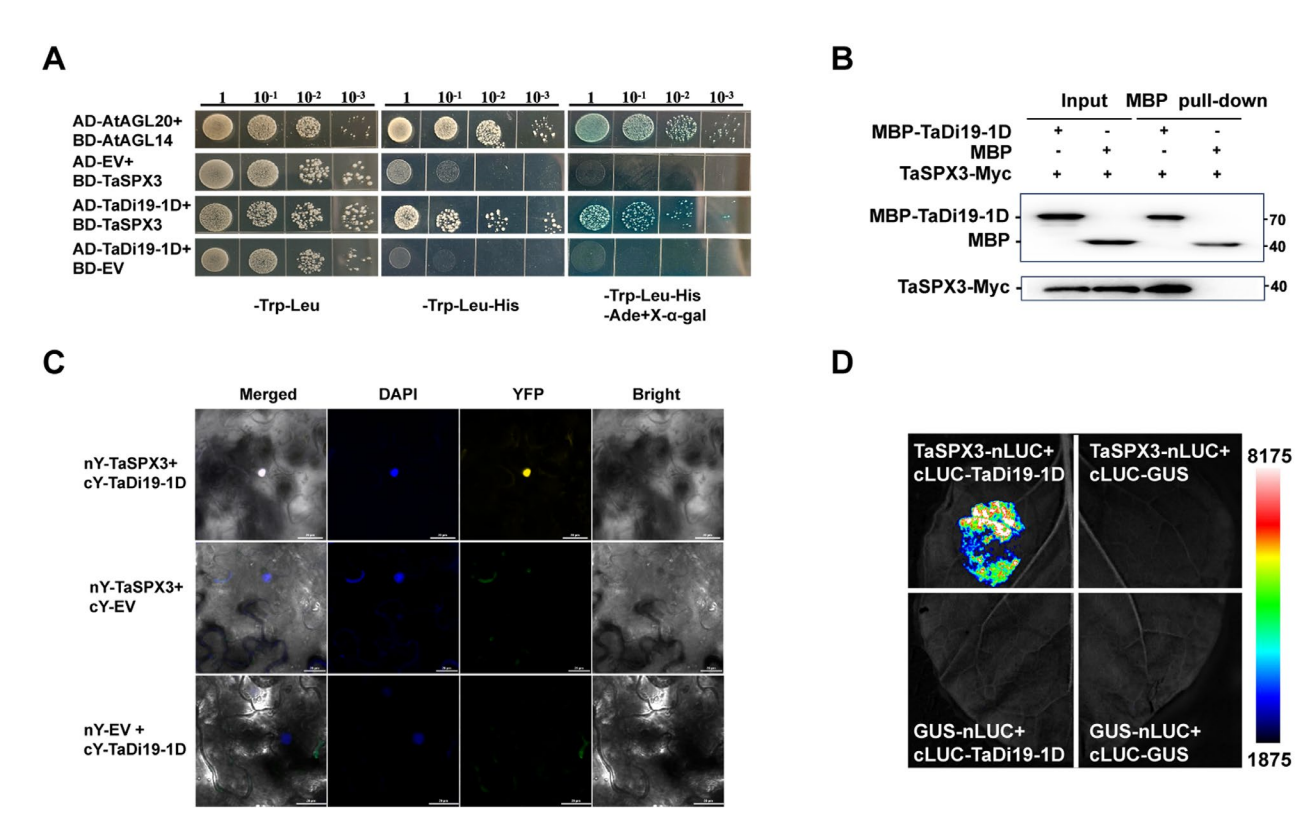


FIGURE 2 | TaSPX3 interacts with TaDi19-1D. (A) TaSPX3 interaction with TaDi19-1D in yeast two-hybrid assays. pGADT7 vector (AD-EV) and pGBKT7 vector (BD-EV) serve as negative controls, whereas AtAGL20/AtAGL14 are positive controls. (B) Pull-down assay showing the interaction between TaSPX3 and TaDi19-1D. Western blot analysis was executed on the recombinant protein mixture eluted from MBP beads, using anti-Myc and anti-MBP antibodies for detection. (C) Bimolecular fluorescence complementation assay detects interaction between TaSPX3 and TaDi19-1D in *Nicotiana benthamiana* leaves. DAPI staining was used to visualise the nuclei, with a scale bar representing 20 μm. (D) Luciferase complementation validation of TaSPX3 and TaDi19-1D interaction. GUS-nLUC and cLUC-GUS were used to establish negative controls.

in the silenced plants (Figure 3D and Figure S7B). Upon inoculation with Pt15, TaDi19-silenced plants exhibited significantly enhanced resistance compared to that of BSMV:y controls. At 10 dpi, the silenced plants developed smaller urediniospore pustules, with more pronounced chlorosis surrounding the infection sites (Figure 3C and Figure S7A). Fungal biomass quantification revealed a marked decrease in Pt15 colonisation in both Fielder and ZM9023 backgrounds (Figure 3E and Figure S7C). Microscopic examination further supported these observations, showing delayed hyphal growth and reduced infection area in the silenced plants (Figure 3F-H and Figure S7D,E). Transcriptional profiling demonstrated that TaPR1, TaPR2 and TaPR5 were significantly upregulated in TaDi19-silenced plants even prior to pathogen challenge (0hpi), with further induction at 24hpi (Figure 3I-K and Figure S7F-H). These findings establish TaDi19 as a negative regulator of wheat immunity against Pt, whose suppression primes defence responses through the constitutive activation of PR genes. The consistent resistance phenotype across cultivars suggests a conserved regulatory role for TaDi19 in wheat-pathogen interactions.

2.7 | TaSPX3 Antagonises TaDi19-1D-Mediated Transcriptional Repression of *PRPR* Genes

Previous studies have established that the Di19 family of zinc-finger transcription factors recognises the conserved TACA(A/G)T (DIBS) motif (Liu et al. 2013). We first confirmed

the transcriptional activation capacity of TaDi19-1D using a yeast two-hybrid assay (Figure S8). Bioinformatics analysis identified multiple DIBS elements within the 2kb promoter regions of TaPR1, TaPR2, TaPR5 (designated TaPR1-pro, TaPR2-pro, TaPR5-pro; Table S2), suggesting their potential regulation by TaDi19-1D. Using yeast one-hybrid assays, we demonstrated that TaDi19-1D physically associates with all three TaPR promoters, as evidenced by colony growth on selective media and intense β -galactosidase activity (Figure 4A). Electrophoretic mobility shift assays further confirmed the specific in vitro binding of recombinant TaDi19-1D to biotin-labelled TaPR promoter probes. These interactions were competitively inhibited by unlabelled WT probes but not by mutated variants (Figure 4B–D), establishing TaDi19-1D as a direct transcriptional regulator of these defence genes.

Dual-luciferase reporter assays in *N. benthamiana* revealed that TaDi19-1D strongly suppressed TaPR-pro:LUC expression and dramatically reduced luciferase activity compared to that of empty vector controls. Notably, this repression was significantly attenuated when TaSPX3 was co-expressed with TaDi19-1D (Figure 5A–D). Mechanistic studies using β -galactosidase assays in yeast showed that, while TaDi19-1D alone enhanced TaPR-pro:LacZ reporter activity approximately 2–3-fold, co-expression of TaSPX3 significantly diminished this activation (Figure 5E–G), indicating TaSPX3 interferes with TaDi19-1D's DNA-binding capacity. Taken together, our data demonstrate that TaSPX3 physically interacts with TaDi19-1D and alleviates the transcriptional repression of TaPR1, TaPR2, TaPR5.

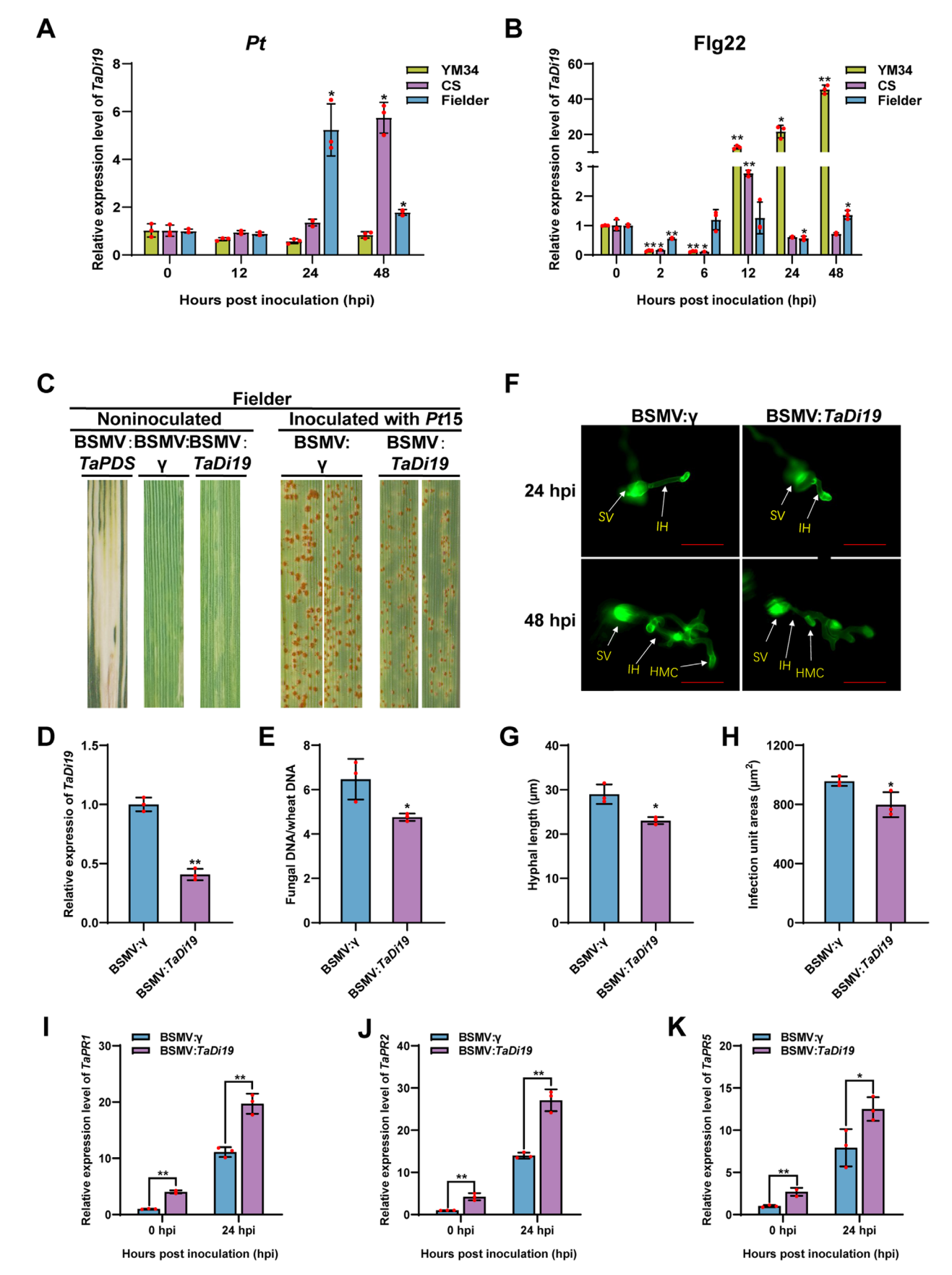


FIGURE 3 | Legend on next page.

FIGURE 3 | TaDi19 silencing increases wheat resistance to leaf rust in Fielder. (A, B) Expression patterns of TaDi19 in wheat leaves during Pt infection (A) and flg22 treatment (B). Leaf samples from CS, Fielder (compatible interaction), YM34 (incompatible interaction) following inoculation with Pt15 were collected at 0, 12, 24, 48 hpi. qRT-PCR was used to test the relative expression levels from three biological replicates. Asterisks indicate significant differences between the column and 0 hpi of the corresponding variety using Student's t-test (*p < 0.05, **p < 0.01). (C) BSMV-induced transient silencing of TaDi19 increases resistance to leaf rust in Fielder. Disease symptoms were observed at 10 dpi. (D) Relative expression of TaDi19 in the inoculated leaves at 0 hpi was assessed using qRT-PCR with Ta26S as the internal control. (E) The fungal biomass in (C) was estimated using qPCR. (F) Inhibited Pt growth in TaDi19-silenced leaves at 24 and 48 hpi. Scale bar, $20 \, \mu \text{m}$. (G, H) Hyphal length at 24 hpi and infection areas at 48 hpi were evaluated using Image J software. Means ± SD were calculated from 30 infection sites of three independent biological repeats. (I–K) The relative expression levels of TaPRs in BSMV:TaDi19 leaves at 0 and 24 hpi were determined. All data are presented as means ± SD. Asterisks above the connecting columns indicate significant differences in the figures (*p < 0.05, **p < 0.01, Student's t-test).

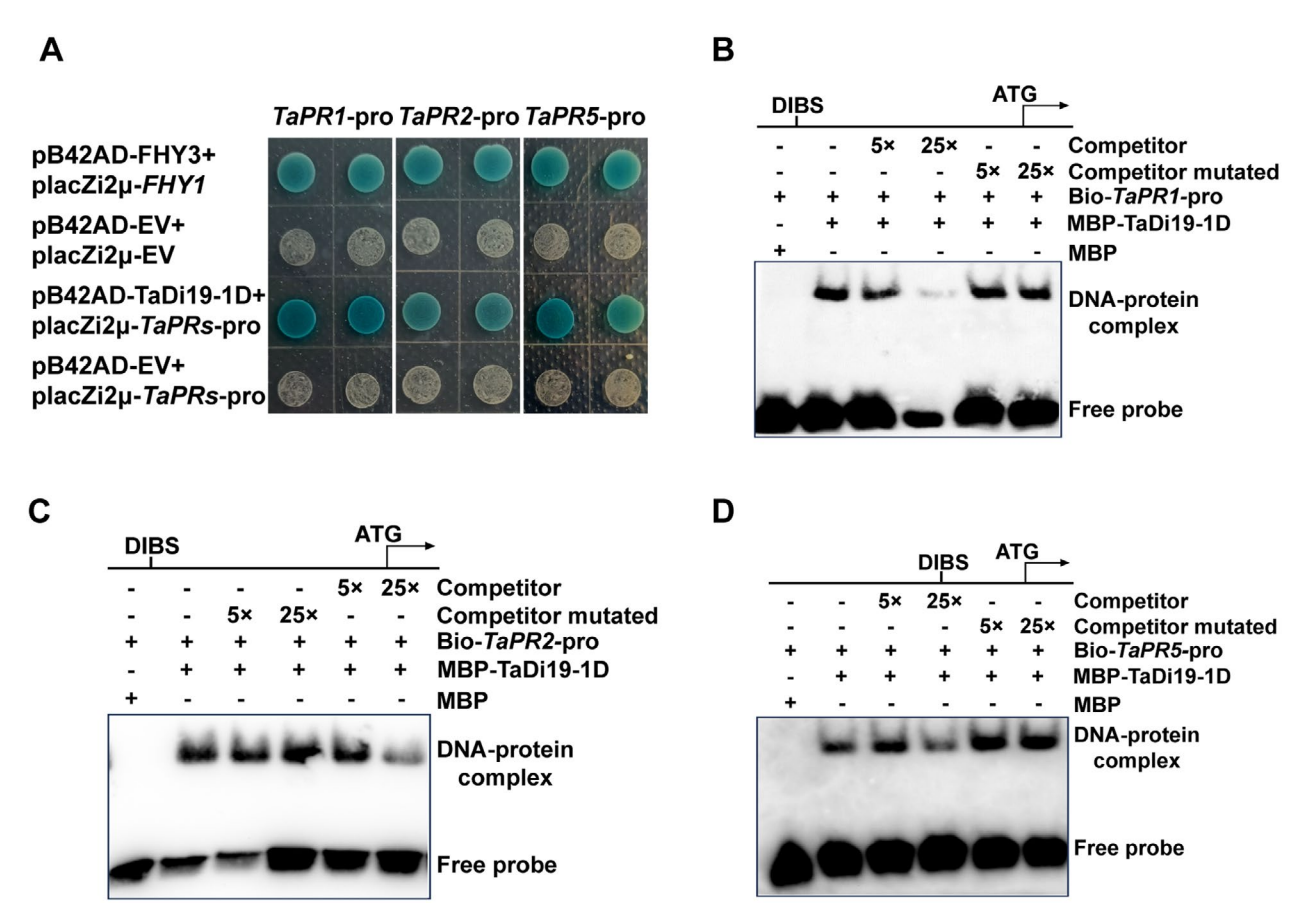


FIGURE 4 | TaDi19-1D targets the *TaPRs* promoter. (A) Yeast one-hybrid assays showing the interaction between TaDi19-1D and the *TaPRs* promoter. Negative controls were established using empty vectors (pB42AD-EV/placZi-EV). (B–D) Gel-shift assay indicating the binding of TaDi19-1D to *TaPRs*-pro in vitro. The formation of a DNA–protein complex is evidenced by the band shift caused by TaDi19-1D binding to the biotin-labelled probe of *TaPRs*-pro. A competitive protein–DNA binding assay was performed using unlabeled WT probe and unlabeled mutant probe (5× and 25×).

2.8 | Mechanistic Model of the TaSPX3-TaDi19-TaPRs Regulatory Network in Wheat Immunity

Our findings establish a comprehensive model in which the dynamic interplay between TaSPX3 and TaDi19 fine-tunes wheat resistance to leaf rust by modulating the expression of PR genes (Figure 6). Upon *Pt* infection, pathogen recognition triggers coordinated changes in *TaSPX3* and *TaDi19* expression, creating a balance that is critical for defence regulation. In *TaSPX3*-overexpressing plants, the increased abundance of TaSPX3 leads to the sequestration of TaDi19 through physical interactions, thereby reducing the pool of unbound TaDi19 available for transcriptional repression. This molecular interaction alleviates

TaDi19-mediated suppression of *TaPR1*, *TaPR2*, *TaPR5*, resulting in their constitutive activation and enhanced resistance. Mechanistically, TaSPX3 interferes with TaDi19's binding to DIBS motifs in *TaPR* promoters, preventing transcriptional repression. Conversely, in *TaSPX3*-silenced plants, a reduction in TaSPX3 levels leads to the accumulation of free TaDi19, which intensifies its repressive effect on *TaPR* promoters. The resulting suppression of PR gene expression renders plants more susceptible to fungal infections.

This regulatory module operates through multiple integrated mechanisms: TaSPX3 post-translationally controls TaDi19's DNA-binding activity, whereas pathogen-induced

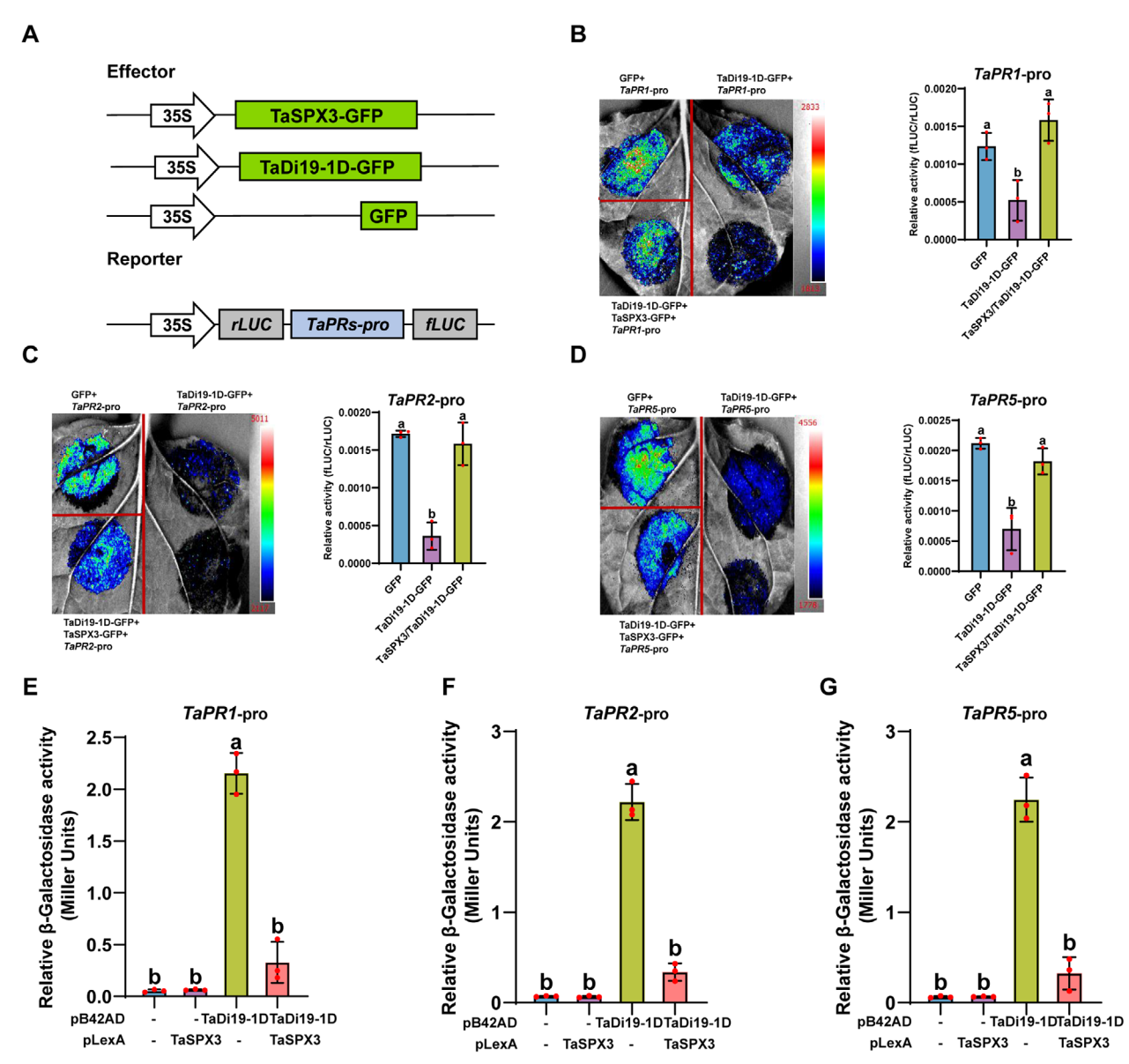


FIGURE 5 | TaSPX3 suppresses TaDi19-1D activity on TaPRs promoters. (A–D) Dual-luciferase reporter assay demonstrating TaDi19-1D represses the TaPRs promoter in N. benthamiana leaves. For quantitative measurements, all infiltrated regions of tobacco leaves were harvested. When two distinct infiltration zones were present, the tissues were combined before processing. The ratio of LUC/REN represents the activity of the TaPR1 (B), TaPR2 (C), TaPR5 (D) promoters in the absence/presence of TaDi19-1D and TaSPX3. (E–G) Quantification of the transcriptional activity assay reveals that TaDi19-1D binds to the TaPRs promoter in yeast. β-galactosidase activity represents TaDi19-1D binding ability to the promoter of TaPR1 (E), TaPR2 (F), TaPR5 (G) in the absence/presence of TaDi19-1D/TaSPX3 and was measured using ONPG as substrate.

transcriptional changes in both components ensure dynamic immune responses. The relative abundance of TaSPX3 and TaDi19, along with their interaction strength, functions as a molecular rheostat to calibrate defense gene expression according to the infection status.

3 | Discussion

SPX domain-containing proteins, which are well characterised in phosphorus homeostasis in model plants, such as *Arabidopsis thaliana* and *Oryza sativa* (Liu et al. 2016; Yang et al. 2024), have recently emerged as important regulators of plant immunity (He et al. 2024). Our study provides the first comprehensive evidence

that TaSPX3 positively regulates wheat resistance to Pt through a novel TaSPX3–TaDi19–TaPRs regulatory module, expanding our understanding of SPX protein functions in plant–pathogen interactions.

The induction of *TaSPX3* expression by both *Pt* infection and flg22 treatment suggested its involvement in wheat–*Pt* interactions and PAMP-triggered immunity (Figure 1A,B). This is further supported by genetic evidence showing that *TaSPX3* overexpression enhances resistance, whereas its silencing increases susceptibility to leaf rust (Figure 1C–E). *TaSPX3* confers broad-spectrum resistance to various *Pt* isolates and two powdery mildew isolates (Figures S3 and S4). Notably, *TaSPX3* overexpression enhanced both the constitutive and

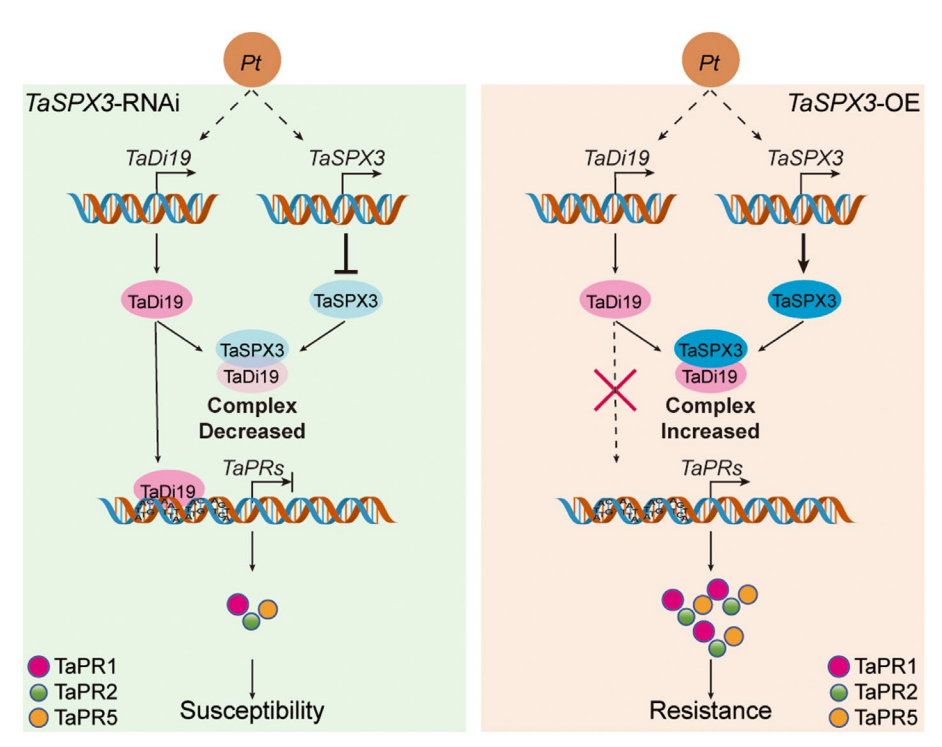


FIGURE 6 | Mechanistic model of TaSPX3–TaDi19-mediated *TaPRs* expression conferring wheat resistance to leaf rust. In wheat, *Pt* infection triggers coordinated expression of *TaSPX3* and *TaDi19*, and the abundance of TaSPX3 and TaDi19 balances *TaPRs* expression to defend against the pathogen. In *TaSPX3*-OE plants, a high level of TaSPX3 facilitates the formation of the TaSPX3–TaDi19 complex. A relatively lower abundance of TaDi19 alleviates its suppression on the downstream *TaPRs*, thereby increasing the enrichment of TaPRs and wheat resistance to leaf rust. By contrast, in *TaSPX3*-RNAi plants, a lower level of TaSPX3 contributes to high TaDi19 abundance, intensifying its repression of *TaPRs* and exacerbating the wheat leaf rust.

pathogen-induced expression of *TaPR1*, *TaPR2*, *TaPR5*, indicating that *TaSPX3* primes the defense system for faster activation. In silenced plants, the absence of a significant reduction in the basal *TaPRs* expression suggests that functional redundancy, possibly through other SPX members or related transcription factors, helps maintain baseline defense without incurring fitness costs, as observed in other systems (Li et al. 2025; Liang et al. 2022). The positive correlation between *TaSPX3* levels and *TaPR1/2/5* expression indicates that *TaSPX3*-mediated resistance operates, at least in part, through the activation of these PR genes (Figure 1G–L).

Our findings reveal an intriguing duality in Di19 protein function. Although previous studies have established Di19 proteins as positive regulators of stress responses (Liu et al. 2013; Zhu et al. 2024), their negative roles in plant development (Dong et al. 2024) and abiotic stress (Du et al. 2023; Yang et al. 2023) responses have also been discovered. We first demonstrated that TaDi19 acts as a transcriptional repressor of defense genes in wheat (Figures 3 and 4) and that this repressive activity is counterbalanced by TaSPX3, which physically interacts with TaDi19 to alleviate its suppression of *TaPRs* (Figures 2 and 5). The discovery of this antagonistic relationship provides a mechanistic explanation of how plants fine-tune their defense responses through competitive protein interactions.

The TaSPX3–TaDi19 module represents a sophisticated regulatory mechanism that integrates pathogen perception with defence gene expression: (1) TaDi19 directly binds to *TaPR* promoters to suppress their expression; (2) TaSPX3 interferes with

this binding through physical interactions; (3) the relative abundance of these proteins determines the amplitude of defence responses. This regulatory circuit allows the dynamic adjustment of immunity based on pathogen challenges and environmental conditions.

Notably, our findings contrast with recent reports showing that SPX proteins are involved in jasmonic acid signalling in rice blast resistance (He et al. 2024; Kong et al. 2021), suggesting a possible evolutionary divergence in SPX-mediated defence mechanisms among cereals. The TaSPX3-TaDi19 pathway appears to represent a distinct strategy for regulating basal immunity through PR gene modulation.

From an applied perspective, our results have important implications for wheat improvement. The conservation of PR proteins across plants (Breen et al. 2017; Han et al. 2023; Li et al. 2024) suggests that manipulating the TaSPX3-TaDi19 module could confer broad-spectrum resistance. Second, the dual roles of SPX and Di19 proteins in both biotic and abiotic stress responses (Kong et al. 2021; Liu et al. 2025, 2024; Zhu et al. 2024) indicate their potential for developing climateresilient varieties. A recent study has demonstrated that pathogenic fungi hijack SPX-PHR signalling through PP-InsP hydrolysis to promote disease development (McCombe et al. 2025). Our identification of TaSPX3 as a positive immune regulator suggests functional convergence in SPXmediated defence. Future studies should investigate whether this TaSPX3-TaDi19 module integrates with broader stressresponse networks.

In conclusion, our work elucidates a previously unrecognised mechanism of wheat immunity involving the competitive regulation of defence genes by TaSPX3 and TaDi19. These findings not only advance our fundamental understanding of plant–pathogen interactions but also provide valuable targets for the molecular breeding of durable and broad-spectrum disease-resistant wheat varieties. The discovery of this regulatory module opens new avenues for investigating how nutrient signalling molecules, such as SPX proteins, integrate with immune responses in crops.

4 | Experimental Procedures

4.1 | Plant Materials and Growth Conditions

YM34, ZM9023, CS are Chinese wheat cultivars with high resistance, moderate resistance, high susceptibility to *P. triticina* isolate *Pt*15, respectively. YM34, CS, Fielder were used to estimate the gene transcript levels in response to *Pt* infection. Fielder was employed to generate the *TaSPX3* overexpression lines (*TaSPX3*-OE) and knockdown lines (*TaSPX3*-RNAi). The Fielder and ZM9023 cultivars were used for transient silencing experiments in wheat. All plants were cultivated in a greenhouse at 21°C with 16 h of light and 8 h of dark. For tillering and seed collection, the plants were grown at 28°C with 16 h of light and at 25°C with 8 h of dark. *Nicotiana benthamiana* was grown at 25°C under 16 h light/8 h dark.

4.2 | Construction of Transgenic Wheat Lines

To construct the TaSPX3-overexpression vector, the full-length coding sequence (CDS) of TaSPX3 was amplified and inserted into the pCUB vector with a His-tag at the C-terminus (pCUB:TaSPX3-His), using a one-step method for recombinant cloning (C115-01, Vazyme, Nanjing, China). To generate an RNAi construct targeting TaSPX3, a 169-bp gene-specific fragment was amplified via PCR using the primers detailed in Table S3 and subsequently integrated into the RNAi vector as inverted repeats (pUbi:TaSPX3-RNAi). The construct was then transformed into wheat cv. Fielder using Agrobacteriummediated transformation, with assistance from the State Key Laboratory for Crop Stress Resistance and High-Efficiency Production at Northwest A&F University, China. Transgenic wheat lines were confirmed through genome- and transcriptlevel validation using PCR and qRT-PCR, respectively. The plasmid was used as a positive control and WT (Fielder) was used as a negative control.

4.3 | Pathogen Inoculation on Wheat Leaves

Pt isolates, Pt15, Pt23, Pt24, were used to evaluate the leaf rust resistance of Fielder and TaSPX3 transgenic lines. For gene expression profiling, Pt15 was inoculated onto the second leaf of wheat seedlings (cv. YM34, CS and Fielder), using an engineered fluid-suspended uredospore method (Sorensen et al. 2016). Transgenic lines and non-transformed controls were challenged at the two-leaf stage (14-day-old plants), and inoculated leaves were collected at 0, 24, 48, 120 hpi for RNA extraction or histological observation. The disease phenotype was monitored, and fungal biomass was

measured at 12 dpi. For the transient silencing assay, plants were inoculated with Pt15 14 days after BSMV infection. The inoculated plants were subsequently maintained in an incubator (24h dark at 21°C, relative humidity of 90%) and then placed in a greenhouse at 21°C with 16h of light/8h of dark cycle.

Bgt isolates JZ-WLQ-3 and SQ-YCS-3 were collected from Henan Province. The seedlings of Fielder and OE lines were inoculated with Bgt isolates and maintained at 22°C, 16 h light/8 h dark cycle with 90% relative humidity in an incubator (Ma et al. 2024). The disease phenotype was determined at 7 dpi.

4.4 | PCR and Quantitative Real-Time PCR (qPCR)

The cetyltrimethylammonium bromide (CTAB) method (Healey et al. 2014) was used for genomic DNA extraction from wheat leaf samples. Fungal biomass measurement in Pt-inoculated leaves was performed through absolute qPCR targeting the PtRTP1 relative to $TaEF1\alpha$ as described previously (Panwar et al. 2017). The total RNA from various tissues was extracted using the Trizol method (DP424, TIANGEN, Beijing, China) (Kiefer et al. 2000) and served as the template for RT-PCR, wherein $1\mu g$ of RNA was reverse-transcribed using PrimeScript II Reverse Transcriptase (TaKaRa, Beijing, China) under manufacturer-specified conditions. The qRT-PCR was performed using SYBR Premix Ex Taq kit (TaKaRa) within a Real-Time PCR instrument (Bio-Rad). The Ta26S gene was used as an internal control. All experiments were performed in triplicates.

4.5 | BSMV-Induced Gene Silencing

To explore the role of TaDi19 in wheat-Pt interactions, we used BSMV-induced gene silencing to target TaDi19. A specific fragment of TaDi19/TaPDS was inserted into the BSMV:γ vector, generating BSMV:TaDi19 and BSMV:TaPDS constructs, respectively. BSMV:y served as the negative control. Linearised plasmids (BSMV:TaDi19, BSMV:TaPDS, BSMV:γ) were transcribed in vitro using T7 RNA polymerase (P1300, Promega, USA) to generate infectious RNAs. The second leaves of two-leaf-stage wheat seedlings were mechanically inoculated with viral RNA mixtures as described previously (Lee et al. 2012). The seedlings were subjected to 90% relative humidity in darkness for 24h and then grown in the greenhouse at 21°C with 16h of light/8h of dark. When plants treated with BSMV:TaPDS exhibited a photobleaching phenotype, the fourth leaf was inoculated with freshly harvested urediniospores of Pt15. Pt-inoculated leaves were sampled at 0, 24, 48 hpi for RNA extraction and histological observations. At 10 dpi, we photographed the disease phenotype and detected fungal biomass. Each inoculation experiment was performed in replicates.

4.6 | Microscopic Analysis of Pathogen Infection

To monitor Pt development in the varying genotypes, the inoculated leaf samples were stained with wheatgerm agglutinin conjugated to Alexa-488 (WGA, Amresco, USA), as previously described (Ayliffe et al. 2011). The substomatal vesicles (SV) and infection hyphae (IH) of Pt were visualised using a positive

fluorescence microscope (ECLIPSE Ni-U, Nikon). Ten infection sites were counted in two randomly selected leaf segments for each experiment. Three independent biological replicates were used for each experiment.

4.7 | Yeast Two-Hybrid Assays

The full-length CDS of TaSPX3 was cloned into the pGBKT7 vector as bait for screening potential interacting proteins from a cDNA plasmid library derived from Pt-infected wheat leaves. Candidate-interacting proteins were subsequently integrated into the pGADT7 vector as prey and co-transformed into the yeast strain Y2HGold with pGBKT7-TaSPX3. AD-AtAGL20/BD-AtAGL14 were constructed as positive controls (Gan et al. 2012). Transformants were cultured in a synthetic dropout medium lacking Leu and Trp (SD/-Leu/-Trp). Individual clones were diluted with stroke-physiological saline solution and introduced onto SD/-Ade/-His/-Leu/-Trp medium supplemented with X- α -Gal. Images were captured after a 4-day incubation at 30°C.

4.8 | Split-Luciferase Complementation Assay

Split-luciferase complementation assays were performed as described previously (Chen et al. 2008; Song et al. 2022). The full-length CDS of *TaSPX3* and *TaDi19-1D* were inserted into the pCambia1300-nLUC and pCambia1300-cLUC vectors to generate TaSPX3-nLUC and cLUC-TaDi19-1D. GUS-nLUC and cLUC-GUS fusion constructs were used as negative controls. The constructs were individually transformed into *Agrobacterium tumefaciens* GV3101 and co-infiltrated into *N. benthamiana* leaves. The infiltrated plants were cultured in an incubator for 48 h at 23°C. The infiltrated leaves were then treated with D-luciferin (BDXB0116, Biodragon) and incubated for 10 min in the dark. Images were captured using a chemiluminescent imaging system (Tanon 5200, China).

4.9 | Subcellular Localisation and Bimolecular Fluorescence Complementation (BiFC) Assays

To perform subcellular localisation in *N. benthamiana* leaves, the full-length CDS of *TaSPX3* and *TaDi19-1D* were respectively cloned into the pCambia1300 and pCambia1305 vectors. For the BiFC assay, *TaSPX3* and *TaDi19-1D* CDS were fused to the pNC-BiFC-Enn and pNC-BiFC-Ecn vectors, respectively. Recombinant plasmids were infiltrated into *N. benthamiana* leaves via *Agrobacterium*-mediated transformation. The signals were observed under confocal microscope (A1HD25, Nikon).

4.10 | In Vitro Pull-Down Assay

For the semi-pull-down assay, the full-length CDS of *TaSPX3* was cloned into the pSuper-Myc vector (TaSPX3-Myc) and transformed into GV3101 for *N. benthamiana* inoculation. Following 48 h post infiltration, total soluble proteins containing TaSPX3-Myc were extracted using NP-40 protein lysis buffer (Beyotime, Shanghai, China). The full-length CDS of *TaDi19-1D* was ligated into the pMAL-c5X vector to generate the MBP-TaDi19-1D

recombinant plasmid. The MBP-TaDi19-1D construct and an empty MBP vector (negative control) were transformed into *Escherichia coli* BL21 (DE3). Protein expression was induced with 0.3 mM isopropylthio- β -galactoside (IPTG) at 16°C with shaking at 150 rpm for 16 h. Protein purification was performed following the Dextrin beads protocol (Cat. No: SA077005, Smart-Lifesciences). Equal amounts of TaSPX3-Myc and MBP-TaDi19-1D or MBP proteins were combined and incubated at 4°C for 3 h with 50 μ L dextrin beads. Proteins retained on the beads were separated using SDS-PAGE and detected with anti-Myc (1:2000) and anti-MBP (1:2000) antibodies. Primers used are listed in Table S3.

4.11 | Transcriptional Activity Assay

For the transcriptional activity assays, the CDS of *TaDi19-1D* was amplified and ligated into the yeast expression vector pGBKT7. BD-TaDi19-1D, BD-EV (negative control), BD-SPL12 (positive control) were individually transformed into yeast strain AH109. Transformants were selected on SD/-Trp medium (Coolaber, China). Then the monoclonal yeasts were transferred onto SD/-His/-Trp medium supplemented with 3 mM 3-AT for 4 days at 30°C. The transcriptional activity was assessed by growth on selective medium.

4.12 | Yeast One-Hybrid

The promoter regions encompassing the TACA(A/G)T elements of *TaPR1*, *TaPR2*, *TaPR5* were amplified and cloned into the pLacZi vector. The CDS of *TaSPX3* and *TaDi19-1D* were inserted into the pLexA and pB42AD vectors, respectively (pLexA-TaSPX3 and pB42AD-TaDi19-1D). In vivo plate assay, these constructs or corresponding empty vectors were co-transformed into the yeast strain EGY48, which was subsequently incubated at 30°C on synthetic dropout medium lacking Trp and Urp. The monoclonal cells were then transferred onto selective medium SD/-Trp/-Ura/Gal/Raf/X-Gal. Primers used are listed in Table S3.

To quantify TaDi19-1D transcriptional activity, liquid culture assays were performed to detect the LacZ activities using onitrophenyl- β -D-galactopyranoside (ONPG; Solarbio) as the chromogenic substrate (Li et al. 2021). The fused plasmid or corresponding empty vector was co-transformed into the yeast strain EGY48. The transformants were selected on SD/-Ura-His-Trp medium at 30°C for 72h. For enzymatic analysis, three individual colonies were inoculated into 1 mL of induction medium (SD/-Ura-His-Trp supplemented with 2% galactose and 1% raffinose) and incubated at 30°C with shaking (200 rpm) for 24h. Cells were pelleted using centrifugation (13000×g, 5 min), and the supernatant was collected to conduct ONPG quantitative assays.

4.13 | Electrophoretic Mobility Shift Assays

The purified MBP-TaDi19-1D fusion protein and MBP were obtained as described above. Probes containing DIBS [TACA(A/G)T] derived from the target promoters were synthesised by Tsingke Biotechnology (Zhengzhou, China), and

the sequences are listed in Table S3. The probes were biotin-labelled using the EMSA Probe Biotin Labelling Kit (GS008, Beyotime). MBP-TaDi19-1D or MBP ($3\mu g$) and biotin-labelled probes were incubated together at 26°C , whereas unlabelled and mutant probes were used as competitors. The experiment was performed using the Chemiluminescent EMSA Kit (GS009, Beyotime) according to the manufacturer's instructions.

4.14 | Dual-Luciferase Reporter Assay

For in vivo dual-luciferase reporter assays, the CDS of *TaSPX3* and *TaDi19-1D* were amplified and integrated into the effector construct pCambia1305 (TaSPX3-GFP and TaDi19-1D-GFP), and the promoter segments (containing the TACA(A/G)T elements) of *TaPR1*, *TaPR2*, *TaPR5* were cloned into the pGreenII0800-LUC vector (0800-*TaPR1*, 0800-*TaPR2*, 0800-*TaPR5*). The plasmids were transferred to *Agrobacterium* GV3101 and then co-transformed into *N. benthamiana*. After 2 days, total proteins from the inoculated leaves were extracted using Lysis Buffer, and luciferase activity was detected using the Dual Luciferase Reporter Gene Assay Kit (11402ES60, Yeasen). The experiments were repeated thrice. Primers used are listed in Table S3.

4.15 | Statistics and Reproducibility

Multiple sequence alignments of the protein sequences were performed using Multalin (http://multalin.toulouse.inra.fr/multalin/) with the default parameters. All experimental data were analysed using GraphPad Prism 8.0 and presented as mean ± standard deviation (SD). Statistical analyses were conducted using two-tailed Student's *t*-test or one-way ANOVA in SPSS 26.0. All experiments were performed two or more times with similar results.

Author Contributions

Wenming Zheng, Pengyu Song, Na Liu, Huimin Qian conceived this study and prepared the manuscript. Huimin Qian, Chuang Li, Yanan Lu, Xue Li, Junyi Zhao, Keyan Wu, Yanyan Zhang designed and performed the experiments. Kun Cheng, Jianping Zhang, Daowen Wang, Wenming Zheng analysed the data and wrote the paper. All authors read and approved the final manuscript.

Acknowledgements

This study was supported by the National Natural Science Foundation of China (32400243), the Henan Provincial Science and Technology Major Project (221100110100), the National Key Research and Development Program of China (2021YFF1000203), the Research start-up fund to topnotch talents of Henan Agricultural University (30500924, 30501347), and the Postdoctoral Fellowship Program of CPSF (GZC20230717).

Conflicts of Interest

The authors declare no conflicts of interest.

Data Availability Statement

The data that supports the findings of this study are available in the Supporting Information of this article.

References

Ali, Y., A. Raza, S. Iqbal, et al. 2022. "Stepwise Regression Models-Based Prediction for Leaf Rust Severity and Yield Loss in Wheat." *Sustainability* 14: 13893.

Ayliffe, M., R. Devilla, R. Mago, et al. 2011. "Nonhost Resistance of Rice to Rust Pathogens." *Molecular Plant-Microbe Interactions* 24: 1143–1155.

Breen, S., S. J. Williams, M. Outram, B. Kobe, and P. S. Solomon. 2017. "Emerging Insights Into the Functions of Pathogenesis-Related Protein 1." *Trends in Plant Science* 22: 871–879.

Chen, H., Y. Zou, Y. Shang, et al. 2008. "Firefly Luciferase Complementation Imaging Assay for Protein-Protein Interactions in Plants." *Plant Physiology* 146: 368–376.

Couto, D., and C. Zipfel. 2016. "Regulation of Pattern Recognition Receptor Signalling in Plants." *Nature Reviews. Immunology* 16: 537-552.

Dong, J., Z. Wang, W. Si, et al. 2024. "The $\rm C_2H_2$ -Type Zinc Finger Transcription Factor ZmDi19-7 Regulates Plant Height and Organ Size by Promoting Cell Size in Maize." *Plant Journal* 120: 2700–2722.

Du, L., L. Ding, D. Tang, H. Zhao, and H. Mao. 2023. "Genome-Wide Analysis of Wheat *Di19* Gene Family and Functional Analysis of *TaDi19-7* in Transgenic *Arabidopsis*." *Environmental and Experimental Botany* 206: 105192.

Gan, Y., A. Bernreiter, S. Filleur, B. Abram, and B. G. Forde. 2012. "Overexpressing the *ANR1* MADS-Box Gene in Transgenic Plants Provides New Insights Into Its Role in the Nitrate Regulation of Root Development." *Plant & Cell Physiology* 53: 1003–1016.

Gultyaeva, E., P. Gannibal, and E. Shaydayuk. 2023. "Long-Term Studies of Wheat Leaf Rust in the North-Western Region of Russia." *Agriculture* 13: 255.

Han, Q., W. Tan, Y. Zhao, et al. 2022. "Salicylic Acid-Activated BIN2 Phosphorylation of TGA3 Promotes *Arabidopsis* PR Gene Expression and Disease Resistance." *EMBO Journal* 41: e110682.

Han, Z., D. Xiong, R. Schneiter, and C. Tian. 2023. "The Function of Plant PR1 and Other Members of the CAP Protein Superfamily in Plant-Pathogen Interactions." *Molecular Plant Pathology* 24: 651–668.

Hassan, A., M. U. Akram, M. A. Hussain, et al. 2022. "Screening of Different Wheat Genotypes Against Leaf Rust and Role of Environmental Factors Affecting Disease Development." *Journal of King Saud University, Science* 34: 101991.

He, Y., Y. Zhao, J. Hu, et al. 2024. "The OsBZR1-OsSPX1/2 Module Fine-Tunes the Growth-Immunity Trade-Off in Adaptation to Phosphate Availability in Rice." *Molecular Plant* 17: 258–276.

Healey, A., A. Furtado, T. Cooper, and R. J. Henry. 2014. "Protocol: A Simple Method for Extracting Next-Generation Sequencing Quality Genomic DNA From Recalcitrant Plant Species." *Plant Methods* 10: 1–8.

Hu, B., Z. Jiang, W. Wang, et al. 2019. "Nitrate-NRT1.1B-SPX4 Cascade Integrates Nitrogen and Phosphorus Signalling Networks in Plants." *Nature Plants* 5: 401–413.

Kiefer, E., W. Heller, and D. Ernst. 2000. "A Simple and Efficient Protocol for Isolation of Functional RNA From Plant Tissues Rich in Secondary Metabolites." *Plant Molecular Biology Reporter* 18: 33–39.

Kong, Y., G. Wang, X. Chen, et al. 2021. "OsPHR2 Modulates Phosphate Starvation-Induced Jasmonic Acid Response and Resistance to Xanthomonas oryzae Pv. Oryzae." Plant, Cell & Environment 44: 3432–3444.

Kumar, S. V., R. Chandan, and P. Pramod. 2024. "Effectiveness of *Lr34* Gene in Reducing Leaf Rust Severity in Wheat Cultivar BRW 934 Transferred Through Marker-Assisted Backcross." *European Journal of Plant Pathology* 169: 601–610.

- Lee, W.-S., K. E. Hammond-Kosack, and K. Kanyuka. 2012. "Barley Stripe Mosaic Virus-Mediated Tools for Investigating Gene Function in Cereal Plants and Their Pathogens: Virus-Induced Gene Silencing, Host-Mediated Gene Silencing, and Virus-Mediated Overexpression of Heterologous Protein." *Plant Physiology* 160: 582–590.
- Legati, A., D. Giovannini, G. Nicolas, et al. 2015. "Mutations in *XPR1* Cause Primary Familial Brain Calcification Associated With Altered Phosphate Export." *Nature Genetics* 47: 579–581.
- Li, H., X. Qin, P. Song, R. Han, and J. Li. 2021. "A LexA-Based Yeast Two-Hybrid System for Studying Light-Switchable Interactions of Phytochromes With Their Interacting Partners." *aBIOTECH* 2: 105–116.
- Li, J., L. Yang, S. Ding, et al. 2024. "Plant PR1 Rescues Condensation of the Plastid Iron-Sulfur Protein by a Fungal Effector." *Nature Plants* 10: 1775–1789.
- Li, W., M. Chern, J. Yin, J. Wang, and X. Chen. 2019. "Recent Advances in Broad-Spectrum Resistance to the Rice Blast Disease." *Current Opinion in Plant Biology* 50: 114–120.
- Li, Z., W. Liu, and Y. Wang. 2025. "VqBGH52 Enhances the Accumulation of Trans-Resveratrol Through Hydrolysis of Trans-Piceid and Resistance to Powdery Mildew in Chinese Wild Grapevine." *Horticultural Plant Journal* ahead of print, March 14.
- Liang, Y., F. Ma, B. Li, et al. 2022. "A bHLH Transcription Factor, SlbHLH96, Promotes Drought Tolerance in Tomato." *Horticulture Research* 9: uhac198.
- Liu, B., W. Xu, Y. Niu, et al. 2025. "TaTCP6 Is Required for Efficient and Balanced Utilization of Nitrate and Phosphorus in Wheat." *Nature Communications* 16: 1683.
- Liu, J., and A. K. M. Ekramoddoullah. 2006. "The Family 10 of Plant Pathogenesis-Related Proteins: Their Structure, Regulation, and Function in Response to Biotic and Abiotic Stresses." *Physiological and Molecular Plant Pathology* 68: 3–13.
- Liu, N., Z. Hu, L. Zhang, et al. 2024. "BAPID Suppresses the Inhibition of BRM on Di19-PR Module in Response to Drought." *Plant Journal* 120: 253–271.
- Liu, N., W. Shang, C. Li, et al. 2018. "Evolution of the *SPX* Gene Family in Plants and Its Role in the Response Mechanism to Phosphorus Stress." *Open Biology* 8: 170231.
- Liu, T.-Y., T.-K. Huang, S.-Y. Yang, et al. 2016. "Identification of Plant Vacuolar Transporters Mediating Phosphate Storage." *Nature Communications* 7: 11095.
- Liu, W. X., F. C. Zhang, W. Z. Zhang, L. F. Song, W. H. Wu, and Y. F. Chen. 2013. "*Arabidopsis* Di19 Functions as a Transcription Factor and Modulates *PR1*, *PR2*, and *PR5* Expression in Response to Drought Stress." *Molecular Plant* 6: 1487–1502.
- Ma, C., X. Tian, Z. Dong, et al. 2024. "An *Aegilops longissima* NLR Protein With Integrated CC-BED Module Mediates Resistance to Wheat Powdery Mildew." *Nature Communications* 15: 8281.
- McCombe, C. L., A. Wegner, L. Wirtz, et al. 2025. "Plant Pathogenic Fungi Hijack Phosphate Signaling With Conserved Enzymatic Effectors." *Science* 387: 955–962.
- Na, L., S. Wenyan, G. Mengxin, et al. 2024. "Phosphate Deficiency Responsive TaSPX3 Is Involved in the Regulation of Shoot Phosphorus in Arabidopsis Plants." *Plant Physiology and Biochemistry* 206: 108215.
- Ngou, B. P. M., M. Wyler, M. W. Schmid, Y. Kadota, and K. Shirasu. 2024. "Evolutionary Trajectory of Pattern Recognition Receptors in Plants." *Nature Communications* 15: 308.
- Panwar, V., M. Jordan, B. McCallum, and G. Bakkeren. 2017. "Host-Induced Silencing of Essential Genes in *Puccinia triticina* Through Transgenic Expression of RNAi Sequences Reduces Severity of Leaf Rust Infection in Wheat." *Plant Biotechnology Journal* 16: 1013–1023.

- Qiu, J., F. Lu, P. Hu, and Y. Kou. 2025. "Hijacking Host Phosphate Sensing: A New Frontier in Plant-Pathogen Warfare." *Science Bulletin* 70: 2909–2911.
- Shi, J., H. Hu, K. Zhang, et al. 2014. "The Paralogous *SPX3* and *SPX5* Genes Redundantly Modulate Pi Homeostasis in Rice." *Journal of Experimental Botany* 65: 859–870.
- Song, P., Z. Yang, C. Guo, et al. 2022. "14-3-3 Proteins Regulate Photomorphogenesis by Facilitating Light-Induced Degradation of PIF3." *New Phytologist* 237: 140–159.
- Sorensen, C. K., T. Thach, and M. S. Hovmoller. 2016. "Evaluation of Spray and Point Inoculation Methods for the Phenotyping of *Puccinia striiformis* on Wheat." *Plant Disease* 100: 1064–1070.
- Sun, T., N. Ma, Y. Jiao, et al. 2024. "TaCAMTA4 Negatively Regulates $\rm H_2O_2$ -Dependent Wheat Leaf Rust Resistance by Activating Catalase 1 Expression." *Plant Physiology* 196: 2078–2088.
- Wang, N., C. Tang, X. Fan, et al. 2022. "Inactivation of a Wheat Protein Kinase Gene Confers Broad-Spectrum Resistance to Rust Fungi." *Cell* 185: 2961–2974.
- Wang, Q., and Y. Kawano. 2024. "The Mutual Regulation Between the Pattern Recognition Receptor OsCERK1 and the E3 Ubiquitin Ligase OsCIE1 Controls Induction and Homeostasis of Immunity." *Scientific Bulletin* 69: 3172–3175.
- Wild, R., R. Gerasimaite, J.-Y. Jung, et al. 2016. "Control of Eukaryotic Phosphate Homeostasis by Inositol Polyphosphate Sensor Domains." *Science* 352: 986–990.
- Yang, S.-Y., W.-Y. Lin, Y.-M. Hsiao, and T.-J. Chiou. 2024. "Milestones in Understanding Transport, Sensing, and Signaling of the Plant Nutrient Phosphorus." *Plant Cell* 36: 1504–1523.
- Yang, Y., R. Ren, A. Karthikeyan, et al. 2023. "The Soybean GmPUB21-Interacting Protein GmDi19-5 Responds to Drought and Salinity Stresses via an ABA-Dependent Pathway." *Crop Journal* 11: 1152–1162.
- Yu, X. Q., H. Q. Niu, C. Liu, H. L. Wang, W. Yin, and X. Xia. 2024. "PTI-ETI Synergistic Signal Mechanisms in Plant Immunity." *Plant Biotechnology Journal* 22: 2113–2128.
- Zhang, L., C. Shi, L. Li, et al. 2020. "Race and Virulence Analysis of *Puccinia triticina* in China in 2014 and 2015." *Plant Disease* 104: 455–464.
- Zhang, R., B. Li, X. Li, and W. Shang. 2021. "Silencing the Expression of *TaSPX3* by VIGS Decreases the Resistance of Wheat to Leaf Rust (*Puccinia recondite f. sp. Tritici*)." *Journal of China Agricultural University* 26: 26–32.
- Zhao, J., and Z. Kang. 2023. "Fighting Wheat Rusts in China: A Look Back and Into the Future." *Phytopathological Research* 5: 1–30.
- Zhu, M., T. Zhong, L. Xu, et al. 2024. "The ZmCPK39-ZmDi19-ZmPR10 Immune Module Regulates Quantitative Resistance to Multiple Foliar Diseases in Maize." *Nature Genetics* 56: 2815–2826.

Supporting Information

Additional supporting information can be found online in the Supporting Information section. **Figures S1–S8:** pbi70402-sup-0001-FiguresS1-S8. zip. **Tables S1–S3:** pbi70402-sup-0002-TablesS1-S3.xlsx.